論文 / 著書情報
Article / Book Information

Title	REAL-TIME EXECUTING SOURCE LOCATION SYSTEMAPPLICABLE TO ANISOTROPIC THIN STRUCTURES
Authors	YU KUROKAWA, YOSHIHIRO MIZUTANI, MASAMI MAYUZUMI
Citation	Journal of Acoustic Emission, Vol. 23, , pp. 224-232
Pub. date	2005, 1

REAL-TIME EXECUTING SOURCE LOCATION SYSTEM APPLICABLE TO ANISOTROPIC THIN STRUCTURES

YU KUROKAWA, YOSHIHIRO MIZUTANI and MASAMI MAYUZUMI
Department of Mechanical Sciences and Engineering, Tokyo Institute of Technology,
Ookayama, Meguro, Tokyo 152-8552, Japan.

Abstract

In this study, we developed a real-time executing source location system for anisotropic thin structures such as CFRP (Carbon Fiber Reinforced Plastics) tanks. The system consists of AE sensors, an A/D converter on a PC and a computer with proprietary software. We suggest two algorithms to realize the real-time executing source location. The first algorithm is a frequency filtering algorithm utilizing a fast continuous wavelet transform. The second algorithm is a fast source location calculation algorithm for unidirectional anisotropic structures. In the second algorithm, the affine coordinate transform is used. The calculation time for each source location is reduced to 1ess than 15 ms with reasonable accuracy.

1. Introduction

The fracture monitoring of CFRP (Carbon Fiber Reinforced Plastics) is important for assuring structural reliability. AE testing is one of the most effective methods for monitoring fracture. The AE source location can be estimated by considering the arrival times and the velocity of the AE signals. However, special techniques are required for conducting the source location on anisotropic thin structures. The AE in thin plates, such as CFRP structures, propagates as Lamb waves and its velocity depends on the frequency [1]. Due to its dispersive nature, it is difficult to determine the arrival time from the AE waveform. Furthermore, in anisotropic structures, the velocity of the AE has an orientation dependence due to the structural anisotropy. The orientation dependence needs to be taken into account for precise source location to be achieved.

Several papers [2-7] dealing with the source location on anisotropic materials or thin plate-like CFPR structures have been reported so far. For example, Promboon [2] and Blahacek [3] used neural networks for the source location. This method could be adopted without understanding the elastic wave propagation characteristics in the material, but the network needs learning before the utilization. Kwon et al. [6] utilized wavelet and inverse wavelet transform for locating pencil-lead breaks on aluminum and cross-ply CFRP plates. This method improves the source location accuracy, but the anisotropy issue remains unresolved. In order to overcome these problems, Yamada et al. [7] have used the wavelet transform as a frequency filter for determining the arrival time of AE signals. However, the wavelet transformation calculation required for this method is time consuming. Another problem is that the source location is estimated by scanning the virtual source. The method required an iterative calculation at a significant computational cost. For these reasons, the source location algorithm for anisotropic thin structures had been found to be less than suitable for real-time execution. Therefore, we introduced two new algorithms for speeding up both the frequency filtering and the source location calculation.

Figure 1 shows a schematic image of our final goal. The AE sensors are mounted on a CFRP tank during a field test and staff monitors AE during the test. The source location is displayed on a computer screen simultaneously with the generation of AE. The two new algorithms proposed in this study are used in the analysis software and enable real-time source location.

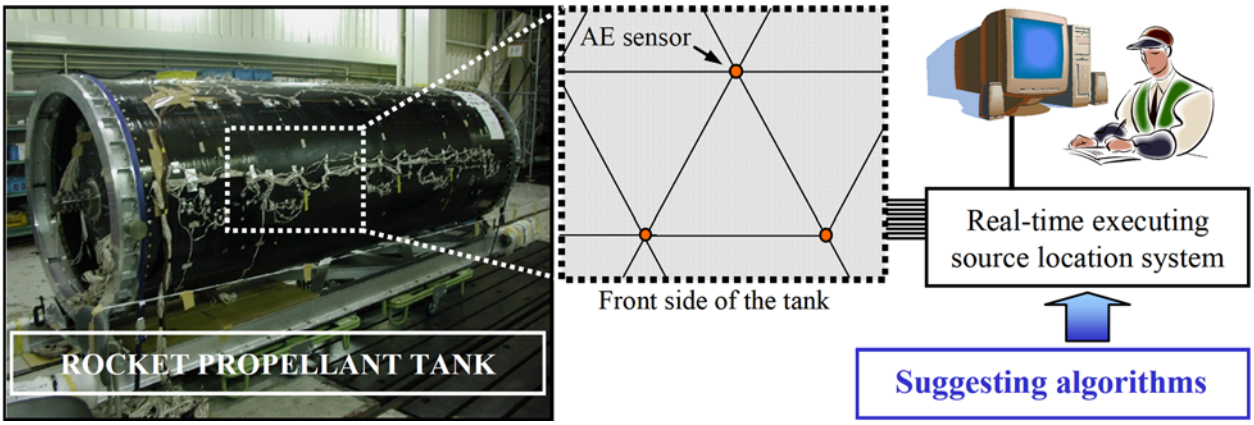

Fig. 1 Schematic image of our final goal

2. Acceleration of the Source Location Calculation

In this study, we suggest two new algorithms for accelerating the source location calculation. One is a new frequency filtering algorithm using the fast continuous wavelet transform. This algorithm enables the immediate extraction of the specific frequency component from the Lamb wave AE. The other algorithm is a new source location algorithm utilizing an affine coordinate transform. This algorithm also shortened the calculation time for source location.

2.1 Fast Frequency Filtering Algorithm

In the source location calculation, the continuous wavelet transform is used as a frequency filter. The general wavelet transform of real function *f(t)* is defined as

$$W(a,b)=\frac{1}{\sqrt{a}}\int_{-\infty}^{\infty} f(t)\psi^{*}\left(\frac{t-b}{a}\right)dt \tag{1}$$

where a>0 and the superscript * denotes a complex conjugation. The analysis function for the wavelet transform can be defined as in equation (2).

$$\psi_{a,b}(t)=\frac{1}{\sqrt{a}}\psi\left(\frac{t-b}{a}\right) \tag{2}$$

Its elements are generated by shifting and scaling a mother wavelet $\psi(t)$. The parameters *a* and *b* stand for the scale and shift of the mother wavelet. The calculation of equation (1) is time consuming because the iterative calculation needs to be performed many times with different values of the parameter b. On the other hand, equation (1) can be transformed into equation (3) utilizing Parseval's theorem [8].

$$W(a,b)=\frac{1}{2\pi}\int_{-\infty}^{\infty}\hat{f}(t)\left\{\sqrt{a}\overline{\hat{\psi}(a\omega)}\right\}e^{i\omega b}d\omega \tag{3}$$

where $\hat{\psi}(\omega)$ donates the Fourier transform of $\psi(\omega)$. Equation (3) can be calculated using the

following steps;

1) Calculate the Fourier transform of $f(t)$ utilizing an FFT.

2) Calculate $\overline{\hat{\psi}(a\omega)}$ using an FFT or other suitable technique.

3) Multiply $\hat{f}(t)$ by $\overline{\hat{\psi}(a\omega)}$. Calculate equation (3) using an Inverse FFT.

A schematic image of the methods stated above is shown in Fig. 2. The general wavelet transform is represented by the convolution of an analytic signal with a mother wavelet function in the time domain (see the left side of Fig. 2). This convolution is time consuming because an iterative calculation is required. On the other hand, the fast wavelet transform used in this study is shown in the right side of Fig. 2. As shown in this figure, the convolution of the two signals is calculated in the frequency domain and the calculation cost is much lower than the general wavelet transform. In this research, the computation time for filtering has been shortened 55 times, from 72 ms to 1.3 ms by this modification.

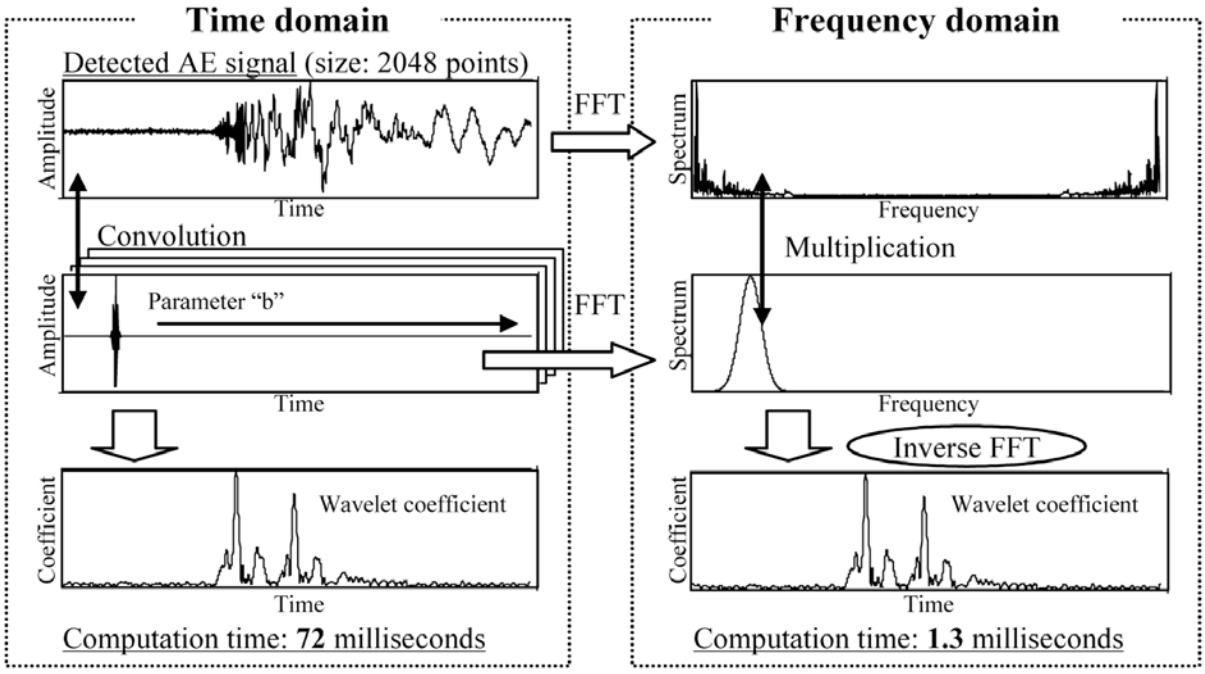

Fig. 2 Comparison of wavelet transform between the time domain and the frequency domain.

2.2 Source Location Algorithm using an Affine Coordinate Transform

The source location on anisotropic thin structures is complicated due to the velocity anisotropy of AE signals. For example, Yamada et al. [7] used the scanning of the virtual source method, as shown in the left side of Fig. 3. The method is computationally intensive and is not suitable for use with real-time source location systems. If velocity anisotropy does not exist, the source location can be calculated immediately using simple simultaneous equations. In our new procedure, the coordinate system is transformed by an affine transform in order to negate the effect of the velocity anisotropy. The right side of Fig. 3 is a schematic representation of this method. The primary requirement is that velocity anisotropy can be approximated by an elliptical function. The new source location algorithm consists of the following steps;

1) Perform an affine coordinate transform using equations (4) and (5) to compensate for the velocity anisotropy effect. The V_0 is the velocity of AE at $\theta = 0°$, V_{90} is at $\theta = 90°$.

According to this process, the location of the sensors: (X_1,Y_1), (X_2,Y_2), (X_3,Y_3) are transformed to (X_1',Y_1'), (X_2',Y_2'), (X_3',Y_3'), respectively.
2) Calculate the source location on the transformed coordinate system using one of the standard AE source location methods. The estimated source location is shown as (x',y') in Fig. 3.
3) Perform an inverse affine transform using equations (6) and (7) for the estimated source by Step 2 as (x',y') and the source location on the original coordinate system is determined as (x,y).

The calculation cost is drastically reduced using this algorithm compared to the scanning virtual source method. In this research, the computation time for source location using this modification has been shortened by three orders of magnitude, from 3.3 s to 3.2 ms.

$$(X',Y')^T = \mathbf{C}(X,Y)^T \tag{4}$$

$$\mathbf{C} = \begin{pmatrix} 1 & 0 \\ 0 & V_0/V_{90} \end{pmatrix} \tag{5}$$

$$(x,y)^T = \mathbf{C}^{-1}(x',y')^T \tag{6}$$

$$\mathbf{C}^{-1} = \begin{pmatrix} 1 & 0 \\ 0 & V_{90}/V_0 \end{pmatrix} \tag{7}$$

3. Specimen and Velocity Anisotropy

For this study, we prepared a 820 mm^L × 300 mm^W CFRP plate ($[90°]_7$) with a 1-mm-thickness aluminum liner. A schematic drawing of the specimen and the source location system are shown in Fig. 4. The total thickness of the composite plate is 2 mm. The Y-axis in Fig. 4 corresponds to the fiber direction of the front CFRP layer. This specimen simulates the propellant tank wall of a future rocket being developed in Japan. We first investigated the orientation dependence of the AE velocity using pulses produced by pencil-lead break on the front surface. We measured the velocity anisotropy every 10° angle (θ) at a particular frequency (f), and approximated it by an elliptical function, $V(f, \theta)$;see Fig. 5. The measured and approximated orientation dependence of the 300-kHz components are shown in Fig. 5 as an example. We subsequently investigated the frequency dependence of the AE signals by utilizing a wavelet transformation by changing the filtering frequency. The frequency dependence of the AE velocity, which we used for source location, is shown in Fig. 6.

4. Source Location System and Experimental Results

The source location experiment used three AE sensors (PAC, type PICO; 4.0 mm diameter). The sensors were mounted on the front surface (CFRP side) at the corners of an equilateral triangle, 200 mm on a side. The AE signals were artificially produced using pencil-lead breaks and steel-ball drops. Outputs of the AE sensors were digitized using an A/D converter on a PC (National Instruments, NI-5122; 14-bit resolution). The sampling frequency and points are 2.5 MHz and 2048 points, respectively. The digitized data is automatically analyzed in the computer and the results are displayed on a computer screen.

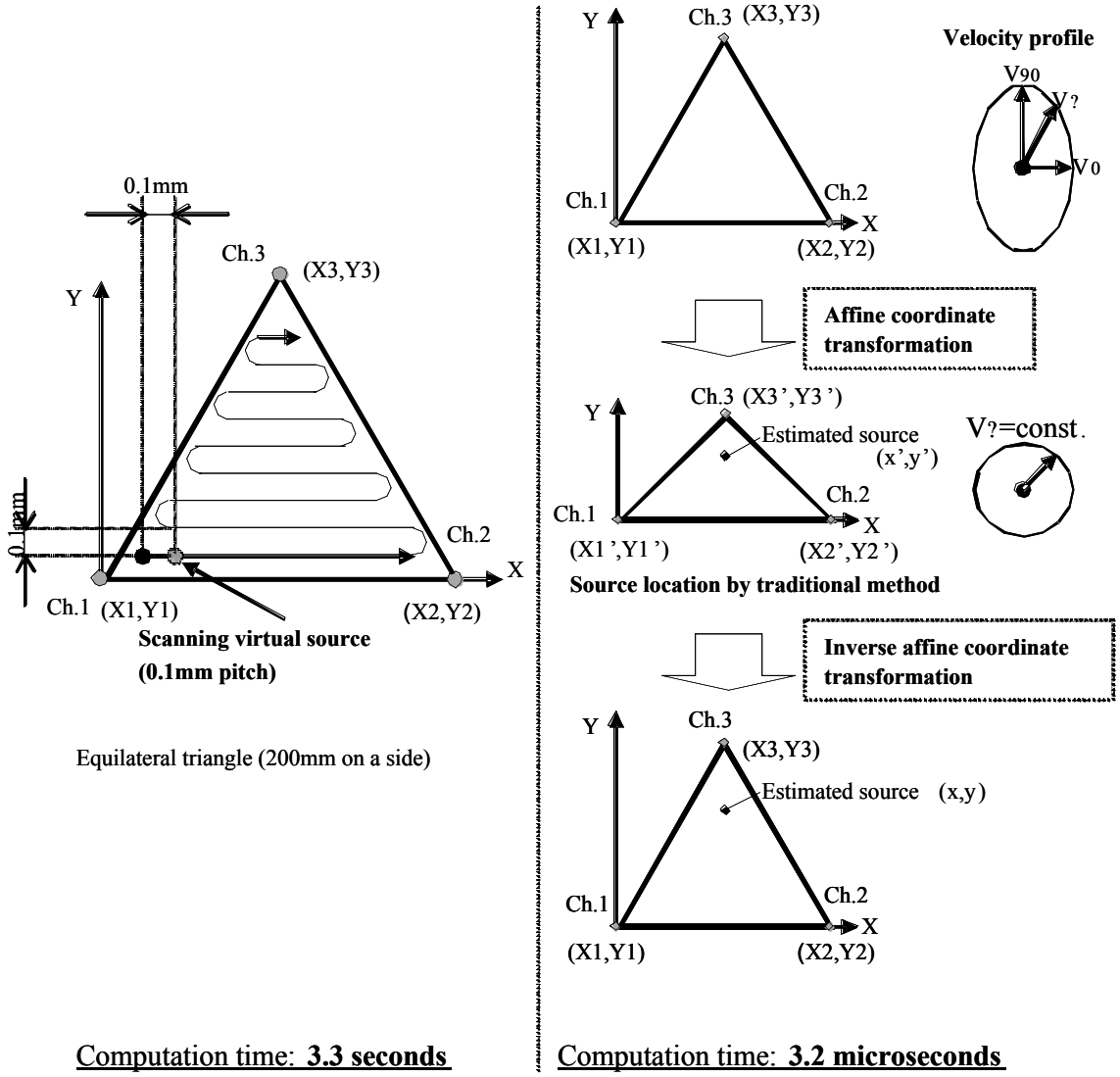

Fig. 3 Comparison of source location methods.

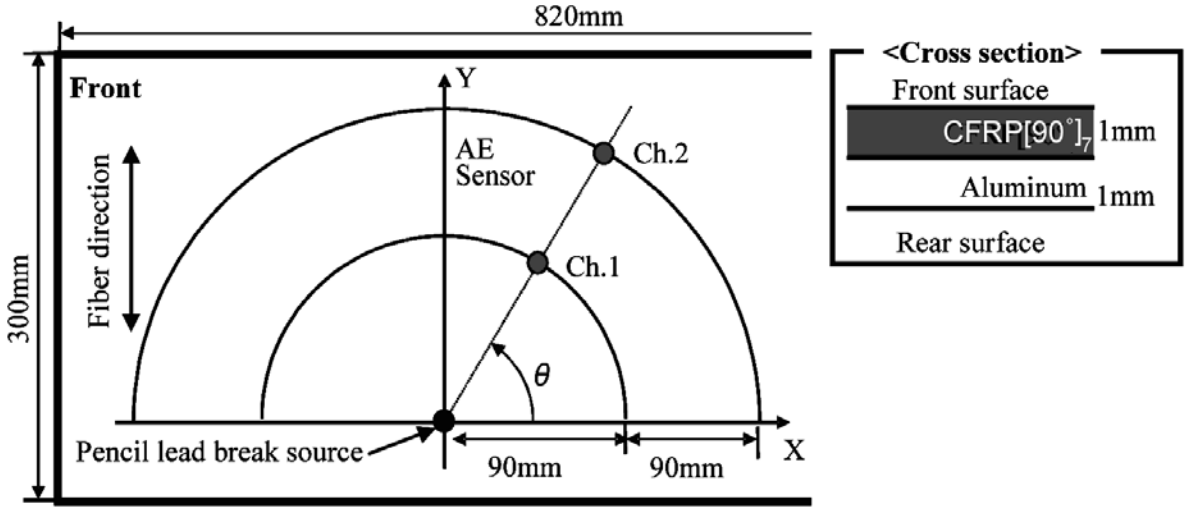

Fig. 4 Schematic illustration of the specimen and the measurement of the orientation and frequency dependence of the AE velocity.

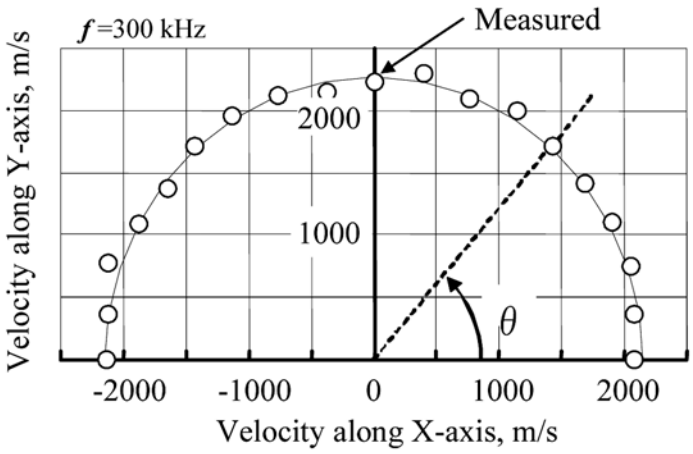

Ellipse Fitting: $V(f,\theta)=\dfrac{V_0 \cdot V_{90}}{\sqrt{V_0^2 \sin^2\theta + V_{90}^2 \cos^2\theta}}$

Fig. 5 Orientation dependence of the AE velocities in the specimen.

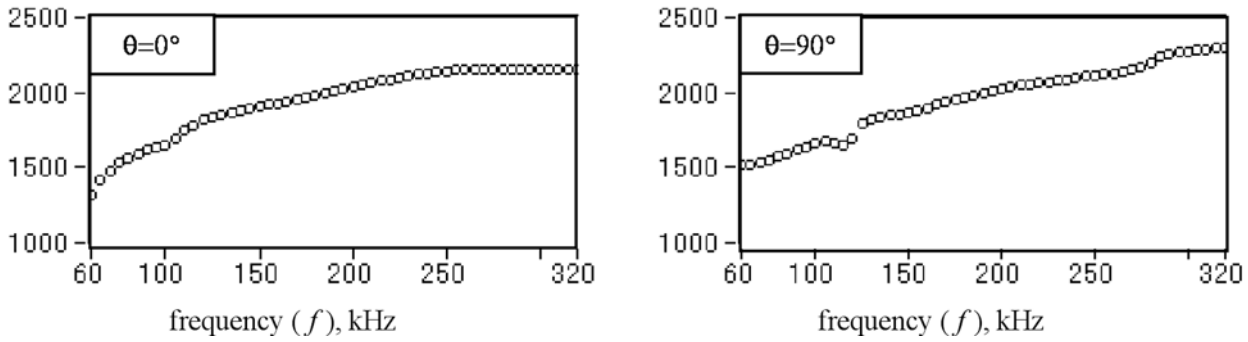

Fig. 6 Frequency dependence of the AE velocity in the specimen.

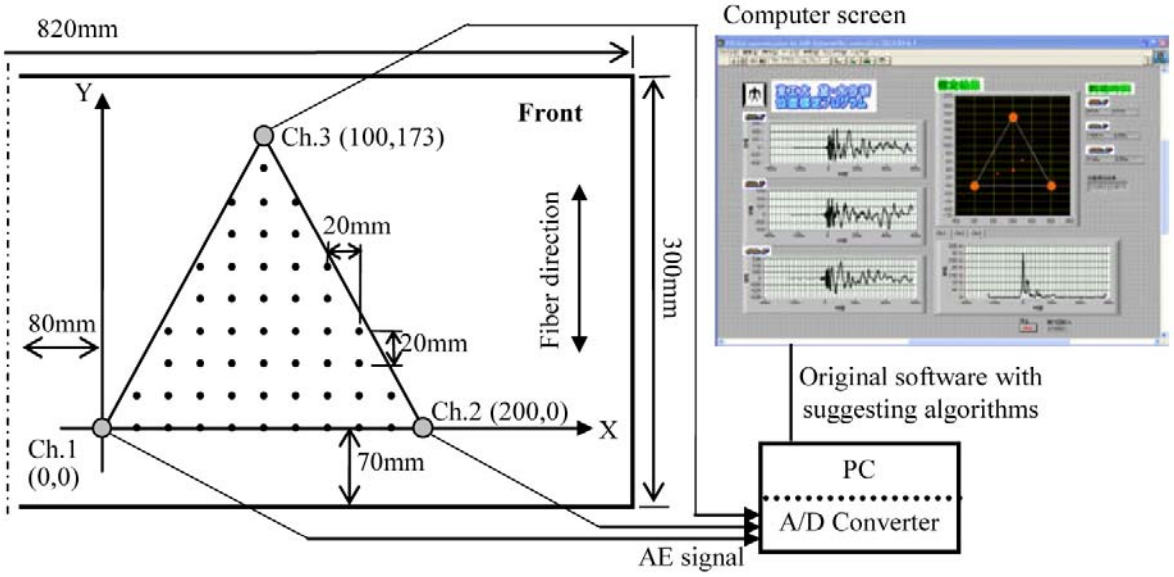

Fig. 7 Schematic illustration of the source location system.

In this study, we conducted the source location using the following steps:

1) Detect the AE signals using three AE sensors.

2) Compare the maximum amplitude of three AE signals and find the weakest signal.

3) Calculate FFT and detect the maximum spectrum. 4)

4) Search the spectrum from 320 kHz to 60 kHz and find frequency *f* that exceeds 4% of the maximum spectrum first. The frequency "*f*" was used for the source location (Step 2 to Step 5 are shown in Fig. 8).

5) Using the frequency "*f*", conduct the wavelet transform for each signal and determine the AE arrival time from the first peak timing of wavelet coefficient.

6) Calculate the source location by the affine transformation algorithm using the arrival time differences.

An example of detected AE signals produced by the pencil-lead break source and the steel-ball drop source at (x,y) = (100,120) [mm] in Fig. 7 are shown in the left side of Fig. 9 and Fig. 10, respectively. Dispersive AE signals propagating as Lamb waves (primary A-mode) were observed. It is difficult to determine the arrival times from the waveform. On the other hand, its wavelet coefficients are shown in the right side of the same figures. The peaks were obtained clearly, and the source location results were (x,y) = (100.6,119.2) and (100.5,121.0) [mm], respectively. The required time for source location is less than 15 ms for any AE sources.

Figure 11 indicates the source location results with pencil-lead break and steel-ball drop sources. The source positions are indicated by squares and the estimated source positions by gray circles in the figure. The maximum error of 6.1 mm and average error of 1.8 mm were obtained for the pencil-lead break source. For the steel-ball drop source, the average error was 3.9 mm and the maximum error was 12 mm. The large error is attributed to the problem of estimating the arrival time from the wavelet results, arising from the lower frequency contents of steel-ball sources.

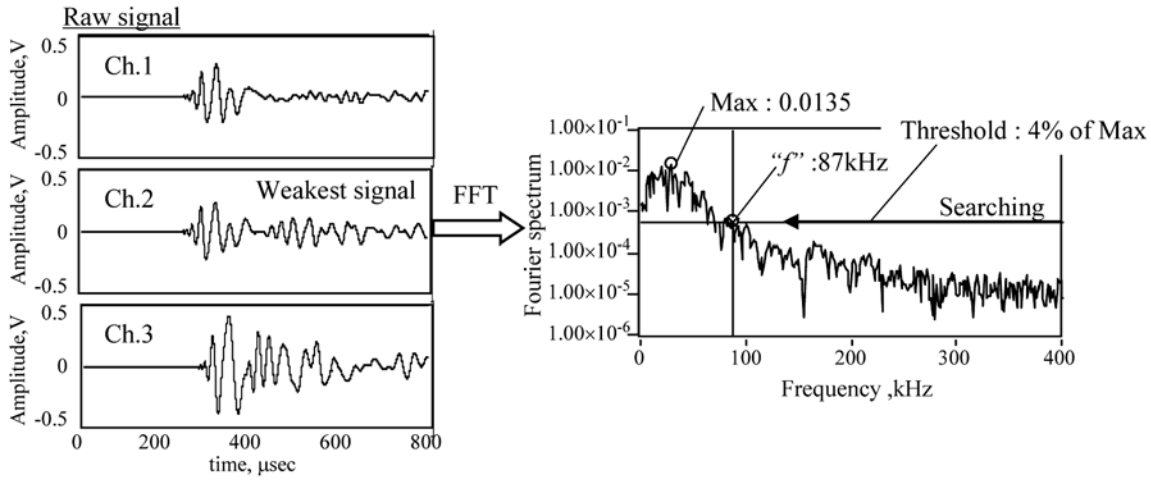

Fig. 8 The method for determining the suitable frequency for source location.

5. Conclusion

We developed a real-time execution source location system applicable to anisotropic thin structures. Two new algorithms for speeding up the source location are proposed. The first algorithm is a frequency-filtering algorithm, which uses a fast continuous wavelet transform. The second algorithm is a fast source location calculation algorithm for unidirectional anisotropic

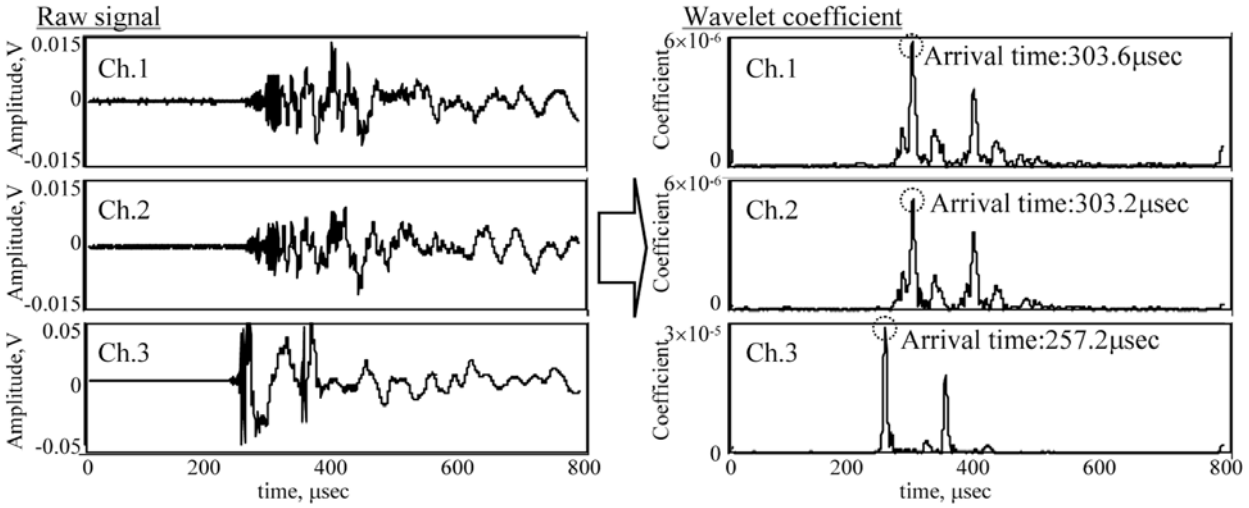

Fig. 9 Example of detected AE signals and the wavelet coefficients produced by pencil-lead break source.

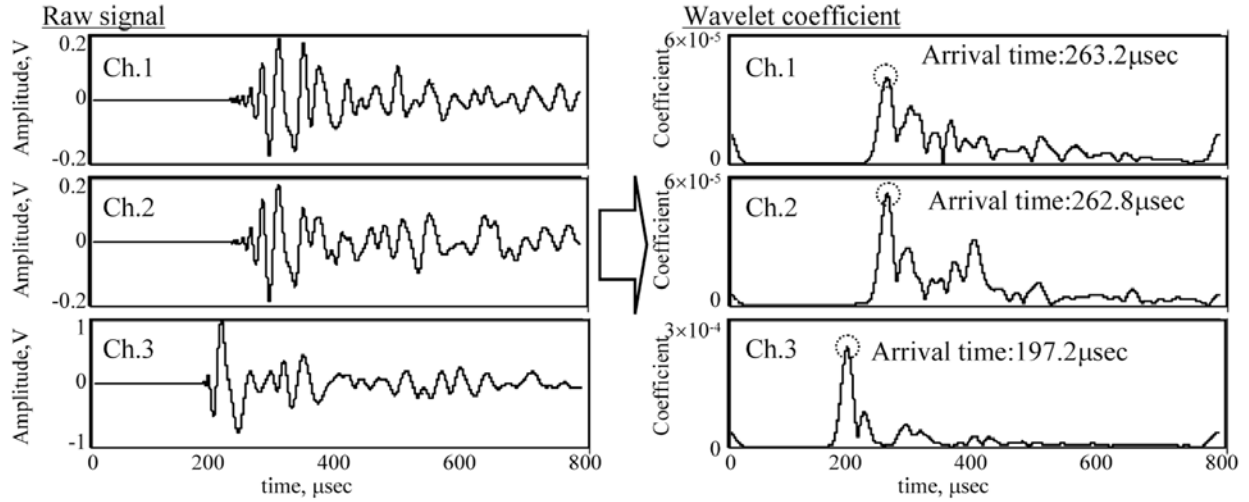

Fig. 10 Example of detected AE signals and the wavelet coefficients produced by steel-ball drop source.

structures. With both improvements, the online monitoring of anisotropic thin structures is now possible. The validity of the developed system is examined using lined CFRP plates. The calculation time for each source location is less than 15 ms with a good location accuracy.

References

1. M.R. Gorman and W.H. Prosser, "AE Source Orientation by Plate Wave Analysis", J. Acoustic Emission, **9**, (1991) 283-288.

2. Y. Promboon and T.J. Fowler, "Source location on fiber reinforced composites", paper presented at 6-th Int. Symp. on AE from Composite Materials, San Antonio, Texas, 1998.

3. M. Blahacek and Z. Prevorovsky, "Probabilistic definition of AE events", European Conference on Acoustic Emission Testing, Prague, 2002, pp. I/63-I/68.

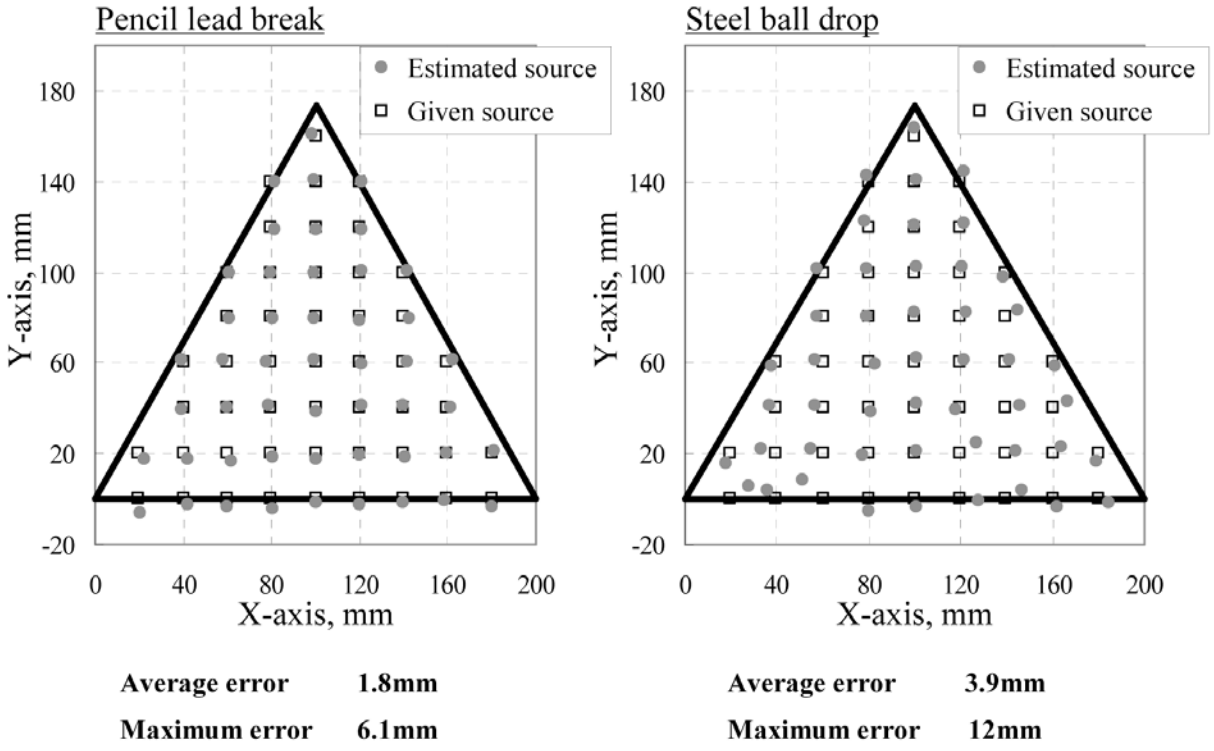

Fig. 11 Source location results for pencil-lead break and steel-ball drop sources.

4. V. Venkatesh and J.R Houghton, "Neural Network Approach to Acoustic Emission Source Location", J. Acoustic Emission, **14** (2), (1996), 61-68.

5. S.M. Ziola and M.R. Gorman, "Source Location in Thin Plates Using Cross-Correlation", J. Acoustic Soc. Am., **90** (5), (1991) 2551-2556.

6. O.Y. Kwon and Y.C. Joo, *Progress in Acoustic Emission VIII*, (1998), JSNDI, Tokyo, pp. 9-17.

7. H. Yamada, Y. Mizutani, H. Nishino, M. Takemoto and K. Ono, J. Acoustic Emission, **18** (2000), 51-60.

8. C.K. Chui, *An Introduction to Wavelets*, Academic Press, (1992), pp. 60-61.